0026-895X/05/6705-1783–1796$20.00
MOLECULAR PHARMACOLOGY
Vol. 67, No. 5
7435/1201295
Mol Pharmacol 67:1783–1796, 2005
Printed in U.S.A.

Developmental Regulation of β-Carboline-Induced Inhibition of Glycine-Evoked Responses Depends on Glycine Receptor β Subunit Expression

Jean-Marie Mangin, Laurent Nguyen, Catherine Gougnard, Grégory Hans, Bernard Rogister, Shibeshih Belachew, Gustave Moonen, Pascal Legendre, and Jean-Michel Rigo

Center for Cellular and Molecular Neuroscience (J.-M.M., L.N., C.G., G.H., B.R., S.B., G.M., J.-M.R.) and Department of Neurology (B.R., S.B., G.M.), University of Liège, Liège, Belgium; Unité Mixte Recherche 7102, Centre National de la Recherche Scientifique, Université Pierre et Marie Curie, Paris, France (J.-M.M., P.L.); Division of Molecular Neurobiology, National Institute for Medical Research, The Ridgeway, Mill Hill, London, England (L.N.); and Department of Physiology, Transnationale Universiteit Limburg/Limburgs Universitair Centrum, Diepenbeek, Belgium (J.-M.R.)

Received September 21, 2004; accepted February 16, 2005

ABSTRACT

In this work, we show that β-carbolines, which are known negative allosteric modulators of $GABA_A$ receptors, inhibit glycine-induced currents of embryonic mouse spinal cord and hippocampal neurons. In both cell types, β-carboline-induced inhibition of glycine receptor (GlyR)-mediated responses decreases with time in culture. Single-channel recordings show that the major conductance levels of GlyR unitary currents shifts from high levels (≥50 pS) in 2 to 3 days in vitro (DIV) neurons to low levels (<50 pS) in 11 to 14 DIV neurons, assessing the replacement of functional homomeric GlyR by heteromeric GlyR. In cultured spinal cord neurons, the disappearance of β-carboline inhibition of glycine responses and high conductance levels is almost complete in mature neurons, whereas a weaker decrease in β-carboline-evoked glycine response inhibition and high conductance level proportion is observed in hippocampal neurons. To confirm the hypothesis that the decreased sensitivity of GlyR to β-carbolines depends on β subunit expression, Chinese hamster ovary cells were permanently transfected either with GlyR α2 subunit alone or in combination with GlyR β subunit. Single-channel recordings revealed that the major conductance levels shifted from high levels (≥50 pS) in GlyR-α2-transfected cells to low levels (<50 pS) in GlyR-α2+β-containing cells. Consistently, both picrotoxin- and β-carboline-induced inhibition of glycine-gated currents were significantly decreased in GlyR-α2+β-transfected cells compared with GlyR-α2-containing cells. In summary, we demonstrate that the incorporation of β subunits in GlyRs confers resistance not only to picrotoxin but also to β-carboline-induced inhibition. Furthermore, we also provide evidence that hippocampal neurons undergo in vitro a partial maturation process of their GlyR-mediated responses.

This work was supported by the Fonds pour la Formation à la Recherche dans l'Industrie et dans l'Agriculture (Belgium), the Fonds National de la Recherche Scientifique (Belgium), the Fondation Médicale Reine Elisabeth (Belgium), the Ligue belge pour la sclérose en plaque (Belgium), Institut National de la Santé et de la Recherche Médicale (France), the Fondation pour la Recherche Médicale (France), the Centre National de la Recherche Scientifique (France), the Association Française contre les Myopathies, and Institut National de la Santé et de la Recherche Médicale-Communauté française de Belgique agreement (to P.L. and J.-M.R.). G.H., S.B., and B.R. are Research Fellow, Research Associate, and Senior Research Associate, respectively, of the Fonds National de la Recherche Scientifique.

J.-M.M., L.N., P.L., and J.-M.R. contributed equally to this work.

Article, publication date, and citation information can be found at http://molpharm.aspetjournals.org.

doi:10.1124/mol.104.007435.

In the mammalian central nervous system, fast inhibitory neurotransmission is mediated by two major classes of ligand-gated channels: $GABA_A$ receptors ($GABA_A$Rs) and strychnine-sensitive glycine receptors (GlyRs) (Moss and Smart, 2001). Whereas GABAergic neurotransmission has a widespread distribution throughout the brain, glycinergic transmission is mainly restricted to the spinal cord and to the brainstem, where it controls motor rhythm generation underlying the locomotor behavior and also coordinates spinal reflexes (Legendre, 2001). However, GlyRs are also present in various upper brain regions (Malosio et al., 1991), includ-

ABBREVIATIONS: $GABA_A$R, $GABA_A$ receptor; GlyR, glycine receptor; DIV, days in vitro; CHO, Chinese hamster ovary; RT-PCR, reverse transcriptase-polymerase chain reaction; DMSO, dimethyl sulfoxide; PBS, phosphate-buffered saline; PBSg, phosphate-buffered saline containing 0.25% gelatin; DMCM, methyl-6,7-dimethoxy-4-ethyl-β-carboline-3-carboxylate; βCCB, *n*-butyl-β-carboline-3-carboxylate; FG7142, *n*-methyl-β-carboline-3-carboxamide; ANOVA-1, one-way analysis of variance; ANOVA-2, two-way analysis of variance; bp, base pair(s).

ing the cerebellum (Virginio and Cherubini, 1997), the cortex (Flint et al., 1998), the striatum (Sergeeva and Haas, 2001), the amygdala (McCool and Farroni, 2001), the hippocampus (Mori et al., 2002; Chattipakorn and McMahon, 2003; Thio et al., 2003), the ventral tegmental area (Ye, 2000), and the substantia nigra (Mangin et al., 2002). In some of these regions, GlyRs do not seem to participate in fast transmission but rather in tonic modulation of excitability (Mori et al., 2002; Chattipakorn and McMahon, 2003).

GlyRs share with the other members of the nicotinic superfamily of ligand-gated channels a pentameric structure (Ortells and Lunt, 1995). Four α subunits (α1–α4) have so far been characterized for the GlyR (Legendre, 2001). They are able to form functional homomeric channels both in vivo (Singer and Berger, 2000; Thio et al., 2003) and in expression systems (Mangin et al., 2003; Beato et al., 2004). Moreover, they carry all the binding sites for GlyR agonists (Legendre, 2001). On the other hand, only one β subunit is known that has no binding sites for GlyR ligands but rather binds the intracellular anchoring protein gephyrin (Schrader et al., 2004). In the adult brainstem and spinal cord, it is now widely accepted that GlyRs mainly consist of $\alpha1\beta$ heteromers with three α1 subunits and two β subunits (Singer and Berger, 2000). As for the majority of ligand-gated channels, a developmental regulation of GlyR subunit expression is known to occur and is associated with changes in the functional properties of the so-formed receptor. In this respect, in the spinal cord and in the brainstem, embryonic GlyRs are mainly α2 homomers that are transiently replaced by $\alpha2\beta$ heteromers around birth ("juvenile" stage) before the switch to the adult form, namely, $\alpha1\beta$ heteromers (Withers and St John, 1997; Tapia and Aguayo, 1998; Singer and Berger, 2000).

Compared with $GABA_A$Rs, fewer modulators of the GlyRs have been characterized (Laube et al., 2002). Among the main antagonists, strychnine is a proconvulsive alkaloid specific for all GlyR variants and picrotoxin, which is a channel blocker of $GABA_A$Rs, is a competitive allosteric antagonist with a higher efficacy at GlyR homomers than at heteromers (Lynch et al., 1995). Other documented modulators at the GlyR include physiological agents (zinc, Suwa et al., 2001; and protons, Chen et al., 2004) and various pharmacological drugs that often also interact with other channels (e.g., anesthetics, alcohols, steroids, dihydropyridines, or tropeines) (Laube et al., 2002).

In a previous study (Rigo et al., 2002), it was mentioned that glycine-induced responses mediated by GlyRs could be reversibly antagonized by β-carbolines in cultured mouse spinal cord neurons 2 to 4 days after plating. β-Carbolines are better known as negative allosteric modulators of the benzodiazepine site of $GABA_A$Rs (Teuber et al., 1999). Because GlyR inhibition by β-carbolines was described in very "immature" neurons, this suggested that β-carbolines could preferentially act on α homomers, the immature form of the receptor.

The goal of our study was to determine whether β-carboline-evoked inhibition of GlyR depends on the expression of GlyR β subunit. By means of electrophysiological, pharmacological, and molecular biology techniques, we demonstrated that β-carbolines are antagonists at α homomers but not at $\alpha\beta$ heteromeric GlyRs. We also showed that cultured hippocampal neurons undergo, as cultured spinal cord neurons, an in vitro maturation characterized by an increased expression of functional heteromeric GlyRs. Part of this work was previously published in abstract form (Rigo et al., 1998).

Materials and Methods

The experiments have been carried out in accordance with the Declaration of Helsinki and conform to the European Community guiding principles in the care and use of animals (86/609/CEE, CE off J n°L358, 18 December 1986), the French decree no. 97/748 (*J Off République Française*, 1987 Oct 20, pp. 12245–12248), and the recommendation of Centre National de la Recherche Scientifique and University Paris VI.

Neuronal Cell Cultures

Spinal cord neurons and hippocampal neurons were obtained, respectively, from 13-day-old and 16-day-old mouse embryos using methods fully described previously (Leprince et al., 1989; Withers and St John, 1997). In brief, spinal cords or hippocampi were carefully dissected and freed of meninges. They were then cut into small fragments that were incubated in 0.25% trypsin and 0.1% deoxyribonuclease in Ca^{2+}-Mg^{2+}-free salt solution for 25 min at 37°C. This was followed by a wash with their culture medium that consisted of Dulbecco's modified Eagle's medium (Invitrogen, Ghent, Belgium) supplemented with 6 g/l glucose (final concentration), 5% (v/v) fetal calf serum (Invitrogen), 10% (v/v) horse serum (Invitrogen), and the N1 supplement (5 μg/ml insulin, 5 μg/ml transferrin, 20 nM progesterone, 100 μM putrescine, and 30 nM selenium). Dissociation was obtained by up and down aspirations through the large tip of a 5-ml plastic pipette placed on the bottom of a conical glass tube. The resulting cell suspension was filtered through a 40-μm nylon sieve. Fifty microliters of the cell suspension was seeded on glass coverslips (10 mm diameter) coated with polyornithine (0.1 mg/ml in distilled water) in the center of 35-mm plastic Petri dishes (NUNC A/S, Roskilde, Denmark) at a concentration of 1.25×10^6 cells/ml. The medium was renewed once weekly, and cells were used for electrophysiological recordings after 2 to 17 days in vitro (DIV). In the results, different culture time periods are differentiated: "young" or "immature" neurons correspond to neurons cultivated for less than 4 DIV (i.e., for 2 to 3 DIV), which are noted "< 4 DIV" in the figures and "old" or "mature" neurons correspond to neurons cultured for more than 7 DIV (i.e., for 8 to 15 DIV for spinal cord neurons and for 10 to 17 DIV for hippocampal neurons), which are noted ">7 DIV" in the figures.

CHO Cell Cultures

Chinese hamster ovary cells (CHO-K1; American Type Culture Collection, Manassas, VA) were cultured in six-well plates in minimal essential medium (Invitrogen) supplemented with 10% (v/v) fetal calf serum (Invitrogen). CHO were subcultured two times per week. For electrophysiological recordings, cells were seeded onto glass coverslips coated with 0.1 mg/ml polyornithine.

RT-PCR and Quantitative RT-PCR

Total RNAs from adult mouse brains and from cultured neurons and transfected CHO cells were extracted and purified using a mini RNeasy kit (QIAGEN, Westburg, The Netherlands). As determined by 260/280 optical density readings, 1 μg of total RNA was reverse-transcribed using primers with oligo(dT) and 200 U of reverse transcriptase (Superscript II; Invitrogen). A 2-μl aliquot of the resulting cDNA reaction, used as template, was added to a 50-μl PCR reaction mixture containing 0.5 μM concentrations of both forward and reverse primers synthesized by Eurogentec (Seraing, Belgium) (Table 1), 0.2 mM concentrations of each dNTP, 1.5 mM $MgCl_2$, and 5 U of *Taq* polymerase (Promega, Leiden, The Netherlands). Moreover, 5% of DMSO was added to the reaction in the PCR mixture containing the β primers. The PCR program was achieved in a PTC 200 instru-

ment (MJ Research, Watertown, MA). After a 3-min denaturation step at 94°C, amplifications were carried out for 33 cycles (94°C for 30 s, 60°C for 15 s, and 72°C for 30 s), followed by a final extension at 72°C for 9 min. Please note that we used 55°C for the annealing of α1 primers. For α3, after a 2-min denaturation step at 94°C, we performed 34 cycles (94°C for 48 s, 58°C for 60 s, and 72°C for 90s) and a final extension step at 72°C for 5 min. The amplification program for β was an initial denaturation step at 95°C for 2 min and then two cycles (94°C for 45 s, 50°C for 30 s, and 72°C for 30 s) followed by two identical cycles, except that the annealing temperature was 52°C, and then followed by two other identical cycles with an annealing temperature of 54°C and then 21 cycles where annealing temperature was 56°C. The β PCR was finished by a final extension step at 72°C for 5 min. Ten microliters of the PCR reaction was analyzed in a 2% agarose gel in Tris-acetic acid-EDTA buffer. Quantitative PCR was carried out using standard protocols with Quantitec SYBR Green PCR kit (QIAGEN). The PCR mix contained SYBR Green mix, 0.5 μM primers (Table 1), 1 ng of DNA template, and nuclease-free water to reach a final volume of 25 μl. Quantitative PCRs were performed on RotorGene RG-3000 (Corbett Research, Westburg, The Netherlands) and analyzed with Rotorgene software (Corbett Research). The percentage of β subunit gene expression by cultured spinal cord neurons was normalized in function of actin gene expression and was compared with the gene expression in 15 DIV spinal cord neurons that was considered as 100%.

GlyR α2 and β Subunit Cloning and Transfection

One microgram of total RNAs extracted from spinal neurons in culture was reverse-transcribed in a 20-μl reaction volume using Superscript (Invitrogen) and oligo(dT) as primers. Two microliters of the obtained cDNA was used as template in a PCR reaction containing 2.5 U of high-fidelity enzyme blend (Roche Diagnostics, Brussels, Belgium), 1.5 mM $MgCl_2$, the forward primer ATCACGGAAACAGGAATGAAC, and the reverse primer CATCTATTTCTTGTGGACATC for the α2A splice variant of the GlyR α2 subunit (GenBank accession no. X61159). The PCR reaction was performed in an MJ Research PTC-200 thermal cycler (after a 2-min denaturation initial step, 10 cycles at 94°C for 15 s, at 50°C for 30 s, and at 72°C for 2 min were followed by 20 cycles at 94°C for 15 s, at 60°C for 30 s, and at 72°C for 2 min with five additional seconds per cycle and a final extension step at 72°C for 2 min). PCR product was purified on agarose gel and cloned in a pCRII-TOPO vector (Invitrogen). The sequence was checked and the GlyR α2 subunit was then subcloned in pTRACER-CMV vector (Invitrogen) in BstXI sites. The various constructs and their orientation were checked by sequencing. The constructs were transfected into CHO cells using the DAC30 lipofection reagent (Eurogentec) selected with Zeocin 500 μg/ml 48 h later (Invitrogen). Selected recombinant CHO cells were then cloned by dilution, and several clones were tested for their expression of functional GlyRs by RT-PCR, immunocytochemistry, and electrophysiology. The clone that was selected for its higher expression level of GlyR α2 subunits is hereafter denoted GlyR-α2. The GlyR β subunit was also cloned by RT-PCR from cultured spinal neuron RNA using primer with an ApaI site underlined (forward, AACGGGCCCGTTTTCAAGATGAAGTTTTCGTTG and reverse: TTCGGGCCCTAAATATATAGACC). The resulting PCR product was purified on agarose gel and cloned in a pCRII-TOPO vector (Invitrogen). The GlyR β subunit was then subcloned in pCDNA3-Myc-His vector in ApaI sites. The various constructs and their orientation were checked by sequencing. The constructs were transfected into CHO-GlyR-α2 cells using the DAC30 lipofection reagent (Eurogentec) and selected with G418 (Geneticin) at 500 μg/ml 48 h later (Invitrogen). Selected recombinant CHO-GlyR-α2+β cells were tested as described above. The selected clone used in this study is hereafter denoted GlyR-α2+β.

Immunocytochemistry

CHO cells were fixed with 4% (v/v) paraformaldehyde in PBS for 10 min at room temperature. Cells were then permeabilized in PBS + 0.3% Triton for 10 min and nonspecific binding was subsequently blocked by a 30-min treatment in a PBS solution containing 0.25% gelatin (PBSg). To reveal the GlyR mAb4a epitope, cells were then immersed in methanol for 10 min at –20°C. Cells were incubated overnight at 4°C with mouse anti-GlyR α subunit mAb4a (staining an epitope common to all GlyR α subunits; Alexis Biochemicals, Lausen, Switzerland) at 1:100 in PBSg. Cells were then incubated during 2 h at room temperature in a rhodamine-conjugated anti-mouse immunoglobulin (Jackson ImmunoResearch Laboratories, West Grove, PA) diluted at 1:500 in PBSg. Three rinses in PBS were performed between all different steps. Preparations were mounted in Vectashield (Vector Laboratories, Burlingame, CA). In the control experiments, where primary antibodies were omitted, no detectable immunofluorescence was observed. Images were acquired using a laser-scanning confocal microscope (MRC1024; Bio-Rad, Hertfordshire, UK).

Electrophysiology

Whole-Cell Recordings and Drugs. Coverslips containing cultured neurons or transfected CHO cells were transferred to the stage of a Zeiss interferential contrast microscope. They were maintained at room temperature (20–25°C) in a recording chamber that was continuously perfused with a physiological saline solution containing 116 mM NaCl, 11.1 mM D-glucose, 5.4 mM KCl, 1.8 mM $CaCl_2 \cdot 2H_2O$, 2.0 mM $MgCl_2 \cdot 6H_2O$, and 10.0 mM HEPES, pH 7.2. Glycine was purchased from UCB Pharma (Brussels, Belgium). GABA, strychnine, picrotoxin, bicuculline methiodide, SR-95531 (gabazine), Ro 15-1788 (flumazenil), methyl-6,7-dimethoxy-4-ethyl-β-carboline-3-carboxylate (DMCM), *n*-butyl-β-carboline-3-carboxylate (βCCB), and *n*-methyl-β-carboline-3-carboxamide (FG7142) were purchased from Sigma-Aldrich (St. Louis, MO). Stock solutions were prepared at 500

TABLE 1
Sequences of primers used for PCR

cDNA	Primer	Size of Product	Reference
		bp	
GlyR α1			
Forward	5′-GTC CCA ACA ACA ACA ACA CC-3′	211	Nguyen et al. (2002)
Reverse	5′-TCC CAG AGC CTT CAC TTG TT-3′		
GlyR α2			
Forward	5′-CTA CAC CTG CCA ACC CAC-3′	182	Nguyen et al. (2002)
Reverse	5′-CTT GTG GAC ATC TTC ATG CC-3′		
GlyR α3			
Forward	5′-GCA CTG GAG AAG TTT TAC CG-3′	309	Thio et al. (2003)
Reverse	5′-AAT CTT GCT GAT GAT TGA ATG TC-3′		
GlyR β			
Forward	5′-GAA GAA CAC TGT GAA CGG CA-3′	228	Nguyen et al. (2002)
Reverse	5′-GGC TTC TTG TTC TTT GCC TG-3′		

times their final concentration in triple-distilled water (GABA, glycine, strychnine, and gabazine) or in DMSO (picrotoxin, flumazenil, DMCM, βCCB, and FG7142). In the latter case, 0.2% DMSO was also included in other conditions, but it did not significantly influence glycine-gated currents (data not shown). All the drugs were applied by means of a local microperfusion system (SPS-8; List Medical Instruments, Darmstadt, Germany). Borosilicate patch-clamp recording electrodes (5–10 MΩ) were made using a Flaming-Brown microelectrode puller (P97; Sutter Instrument Company, Novato, CA). Micropipettes were filled with an intracellular-like solution containing 130.0 mM KCl, 1.0 mM $CaCl_2{\cdot}2H_2O$, 11.1 mM D-glucose, 10.0 mM EGTA, 2.5 mM Na_2-ATP, 2.5 mM Mg-ATP, and 10.0 mM HEPES, pH 7.4. Standard whole-cell recordings were performed with a Bio-Logic RK400 patch clamp. Series resistances (10–20 Ω) were electronically compensated (80–85%), and current traces were filtered at 3 kHz, acquired, and digitized at 0.5 kHz, and stored on a personal computer system. Control of drug application and data acquisition were achieved using an ITC-16 acquisition board (InstruTECH Corporation, Port Washington, NY) and the TIDA for Windows software (HEKA Elektronik, Lombrecht/Pfolz, Germany).

Outside-Out Recordings. Standard outside-out recordings were achieved under direct visualization (Nikon Optiphot microscope). Cells were continuously perfused at room temperature (20°C) with bathing solution (2 ml/min) containing 145.0 mM NaCl, 1.5 mM KCl, 2.0 mM $CaCl_2$, 1.0 mM $MgCl_2$, 10.0 mM HEPES, and 15.0 mM glucose, pH 7.3; osmolarity, 330 mOsM). Patch-clamp electrodes were pulled from thick-wall borosilicate glass (5–10 MΩ). They were fire-polished and filled with 135 mM CsCl, 2 mM $MgCl_2$, 4 mM Na_3-ATP, 10 mM EGTA, and 10 mM HEPES, pH 7.2; osmolarity, 290 mOsM). Currents were recorded using an Axopatch 1D amplifier (Axon Instruments, Foster City, CA) filtered at 10 KHz and stored using a digital recorder (DAT DTR 1201; Sony, Tokyo, Japan). During recordings, values of seal resistance ranged from 2 to 20 GΩ, and patches were recorded during 15 to 30 min after excision. Control and drug solutions were gravity fed into two channels of a thin-walled glass theta tube (2-mm outer diameter; Hilgenberg) pulled and broken at a tip diameter of 200 μm. The drug application was performed by manually translating the patch pipette in front of the drug-containing channel.

Data Analysis

Except when stated otherwise, the results are expressed as mean and S.E.M. For whole-cell recordings, n represents the number of recorded cells. Peak currents in the different experimental conditions were measured and subsequently normalized to the preceding and the following responses (100%) in control conditions. Agonist concentration-response profiles were fitted to the following equation: $I/I_{max} = 1/(1 + (EC_{50}/[agonist])^{nH})$, where I and I_{max}, respectively, represent the agonist-induced current at a given concentration and the maximum current induced by a saturating concentration of the agonist. EC_{50} is the half-maximal effective agonist concentration, and n_H is the Hill slope. Modulator concentration-response curves were fitted by a similar procedure and yielded IC_{50} values being half-maximal inhibitory drug concentrations.

For all experiments, a statistical analysis was performed using either unpaired two-tailed Student's t test between control and experimental conditions or one-way analysis of variance (ANOVA-1) followed by a Dunnett's multiple comparison post tests when significance was reached or two-ways analysis of variance (ANOVA-2) between concentration-response curves (Prism software, version 4.00; GraphPad Software Inc., San Diego, CA). The level of significance was expressed as follows: *, $P < 0.05$; **, $P < 0.01$; ***, $P < 0.001$.

For outside-out recordings, the analysis of the evoked single-channel openings was performed by selecting patches with a low frequency of openings to avoid overlapping events. Single-channel current levels were determined using point-per-point amplitude histograms obtained from recording epochs of 25 to 50 s. Amplitude histograms were fitted with a sum of Gaussian functions, using the least square method (Simplex algorithm). The optimal number of Gaussian functions was determined by comparing the sum of squared errors of the different multi-Gaussian fits. The different conductance levels were defined from the mean current amplitude of each Gaussian function and the theoretical E_{Cl} (−2 mV). The relative proportion of time spent in each level was given by the relative area of each Gaussian function. Open times were analyzed manually using Axograph 4.6 software (Axon Instruments).

Results

β-Carbolines Dose-Dependently Inhibit Glycine-Gated Currents in Spinal Cord Neurons Cultured in Vitro. In the whole-cell configuration of the patch-clamp technique and in voltage-clamp mode at a holding potential of −70 mV, we recorded, in spinal cord neurons cultured for 2–3 DIV, inward currents elicited by bath application (10 s) of GABA and of glycine (Fig. 1, A and B). These inward currents reversed around 0 mV (data not shown), consistent with them being carried mainly by Cl^-, the calculated Nernst equilibrium potential of chloride being 0.6 mV. GABA currents were blocked in the presence of bicuculline methiodide,

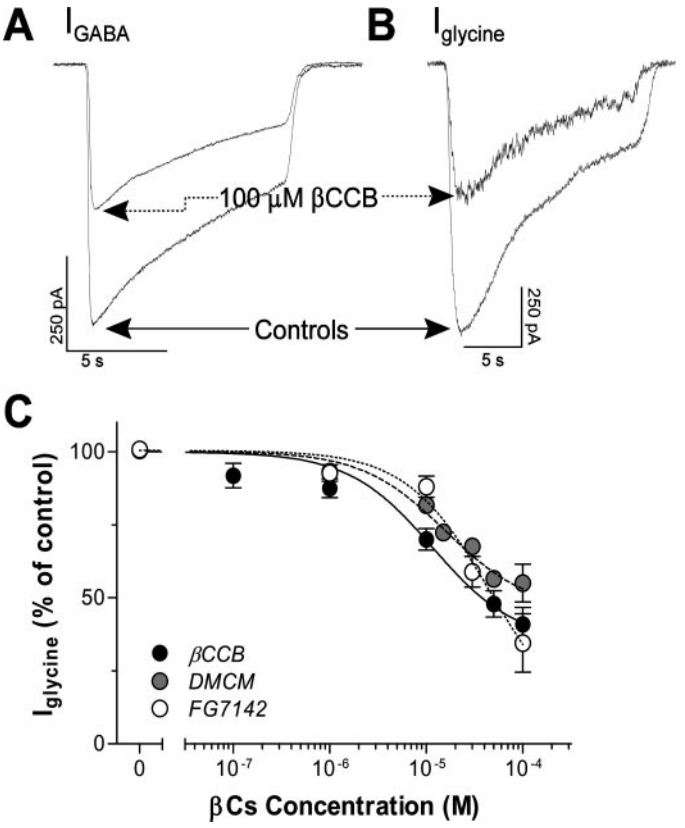

Fig. 1. β-Carbolines reversibly inhibit glycine-induced currents in cultured spinal cord neurons. A and B, same 3 DIV spinal cord neuron was voltage-clamped at a holding potential of −70 mV using the whole-cell patch-clamp technique (see *Materials and Methods*), and currents induced by a 10-s perfusion of 50 μM GABA (A) or a 15-s perfusion of 100 μM glycine (B) alone or in combination with 100 μM βCCB were recorded. βCCB was perfused for 15 s before being coapplied with agonists. A 60-s period was allowed for the washout of drugs. C, currents evoked by 100 μM glycine in 2 to 3 DIV spinal cord neurons were recorded in the presence of increasing βCCB (black filled circles), DMCM (gray filled circles) and FG7142 (empty circles) concentrations. Results are expressed as percentage of glycine-induced currents peak amplitudes in the absence of β-carbolines (mean ± S.E.M., n = 3–15 for βCCB, 3–26 for DMCM, and 4–8 for FG7142).

gabazine, or picrotoxin, and glycine responses were inhibited by strychnine (data not shown), indicating the activation of ionotropic $GABA_A$ and glycine receptors, respectively. Throughout this article, glycine currents were recorded in the presence of 10 μM bicuculline methiodide and GABA responses in the presence of 1 μM strychnine to avoid cross-activation.

As shown in Fig. 1, B and C, and as already reported partially (Rigo et al., 2002), β-carbolines (βCCB, DMCM, and FG7142) dose dependently and reversibly inhibited the current gated by 100 μM glycine, a concentration close to its EC_{50} on these neurons (77.7 ± 13.6 μM; $n = 8$). The level of inhibition by 100 μM βCCB of glycine-induced currents (40.9 ± 5.8% of control; $n = 11$) was in the same order as for GABA-gated responses (38.9 ± 4.8% of control; $n = 5$; $P = 0.8$, unpaired t test), its classic target (Fig. 1, A and B). The plots of the relative current amplitudes as a function of β-carboline concentrations were best fitted by Hill equations yielding half-maximal inhibitory concentrations (IC_{50}) for βCCB of 11.5 ± 2.8 μM (n = 3–15), for DMCM of 15.8 ± 2.8 μM (n = 3–26), and for FG7142 of 46.2 ± 24.2 μM (n = 4–8). Because these concentration-response curves did not statistically differ ($P = 0.09$; ANOVA-2), βCCB was preferentially used to allow intermodel comparisons and hence is illustrated in subsequent figures.

In Vitro Maturation-Dependent Expression of GlyR β Subunit Confers Spinal Cord Neurons Resistance to β-Carboline-Induced Inhibition of Glycine-Gated Currents. It is well known that a developmental switch in GlyR subunits does occur during spinal cord development both in vivo (Becker et al., 1988; Malosio et al., 1991; Legendre, 2001) and in vitro (Withers and St John, 1997; Tapia and Aguayo, 1998), with α2 homomers being progressively replaced by α1β heteromers.

To document and quantify the switch in GlyR subtypes occurring during the maturation of spinal cord neurons in our culture system, we analyzed the single-channel conductance of GlyRs in outside-out patches excised from both 2 to 3 DIV and 11 to 14 DIV spinal neurons. Indeed, GlyRs are known to exhibit multiple conductance states, ranging from 20 to 110 pS, depending on their subunit combination (Bormann et al., 1993). In brief, α homomeric GlyR are able to open in the whole range of conductance states with a main conductance between 90 and 110 pS, whereas the maximal and main conductance state exhibited by αβ heteromeric GlyRs is close to 50 pS (Bormann et al., 1993).

The all-point amplitude histogram of GlyR unitary currents recorded in outside-out patches excised from <4 DIV spinal neurons (Fig. 2B; $n = 9$) shows three distinct peaks at 84, 64, and 43 pS. The 84-pS level is the most frequently observed and represent 58% of the total open time, whereas the 64 pS level and the 43 pS level, respectively, represent 9 and 33% of the total open time. In contrast, the all-point amplitude histogram of GlyR unitary currents observed in >7 DIV spinal neurons (Fig. 2D; $n = 8$) exhibits only one peak at 38 pS. These results show that young (<4 DIV) or immature spinal neurons predominantly express α homomeric GlyRs (>55 pS), which seem to be completely replaced by αβ heteromeric GlyRs in older (>7 DIV) or mature neurons.

In the whole-cell configuration of the patch-clamp technique and in voltage-clamp mode at a holding potential of −70 mV, we then analyzed the changes occurring in GlyR pharmacology during this maturation process. It has already been demonstrated that, when maturing in vitro, spinal cord neuron GlyRs lose their ability to be modulated by picrotoxin (Tapia and Aguayo, 1998). We therefore used picrotoxin sensitivity as a tool to discriminate between GlyR homomers and heteromers. Figure 3A shows that although 10 μM picrotoxin blocks ~50% of glycine currents in 2 to 3 DIV neurons, it only slightly affects the response of 8 to 15 DIV neurons. This was confirmed by the highly significant difference in picrotoxin concentration-response effect between the two maturation stages (Fig. 3B) ($P < 0.001$; ANOVA-2). As shown in Fig. 3, C and D, this change in GlyR pharmacology seems also valid for βCCB inhibition. Indeed, the maximal inhibition by 100 μM βCCB dropped from 40.9 ± 5.8% of control ($n = 11$) in <4 DIV spinal cord neurons to 88.4 ± 4.0% of control ($n = 4$) in >7 DIV neurons ($P < 0.001$; ANOVA-2).

To further determine whether the loss in βCCB sensitivity of spinal cord neuron GlyRs can be related to a switch in GlyR subunit expression, we investigated GlyR subunit expression in immature and mature cultures. As seen in Fig. 3E, both α1 and α2 subunit mRNAs are detected by RT-PCR from the beginning of the culture time period, whereas β subunit messengers are only detected in mature neurons. Moreover, quantitative RT-PCR measurements of β subunit transcripts (Fig. 3F) at different culture times show that their appearance coincides with the progressive loss in both picrotoxin and βCCB sensitivity of spinal cord neuron GlyRs. The 4 to 6 DIV period corresponds to the decaying phase of picrotoxin and βCCB inhibition. Measurements done at this culture maturation stage were thus discarded from all comparisons between immature and mature neurons.

GlyRs of Immature Hippocampal Neurons Are Also Sensitive to β-Carbolines. Although it is tempting to conclude from spinal cord neuron experiments that β-carboline inhibition of GlyR is, like picrotoxin inhibition, caused by the lack of β subunits in immature cultures, we cannot completely rule out the idea that the reduction in β-carboline sensitivity could also result from the known GlyR α subunit swapping (α2 to α1) described in spinal cord. Therefore, we looked for a neuronal cell type known not to express α1 subunits. Hippocampal neurons could fulfill such a model. Indeed, functional GlyRs have been described in the hippocampus in vitro as well as in vivo (Chattipakorn and McMahon, 2002; Mori et al., 2002), both during development and in the adulthood (Malosio et al., 1991; Hogg et al., 2004). Their role therein, especially for what concerns their implication in neurotransmission, remains a matter of debate (Chattipakorn and McMahon, 2002; Mori et al., 2002). Nevertheless, it is well established that they lack α1 subunit expression (Malosio et al., 1991). Indeed, RT-PCR amplification of mRNAs extracted from cultured hippocampal neurons yielded no signal for α1 transcripts (Fig. 5E).

To document a possible functional switch in GlyR subtype in hippocampal neuronal cultures, we first analyzed the single-channel conductance of GlyRs in outside-out patches excised from both 2 to 3 DIV and 11 to 14 DIV hippocampal neurons (Fig. 4). The all-point amplitude histogram of GlyR unitary currents recorded in outside-out patches excised from <4 DIV hippocampal neurons (Fig. 4B; $n = 9$) shows three peaks at 96, 66, and 45 pS. The 96-pS level is the most frequently observed and represents 48% of the total open

time, whereas the 66- and 45-pS levels represent 24 and 33% of the total open time, respectively. In >7 DIV hippocampal neurons, the amplitude histogram (Fig. 4D; $n = 7$) exhibits only two distinct peak at 86 and 45 pS, the 45-pS level being predominant with 77% of the total open time. As observed in immature spinal neurons, these results show that immature hippocampal neurons functionally express a majority of α homomeric GlyRs (>55 pS), which are replaced by $\alpha\beta$ heteromeric GlyRs in mature hippocampal neurons. Nevertheless, contrasting with mature spinal neurons, mature hippocampal neurons seem to maintain the expression of a small fraction of α homomeric GlyRs.

In the whole-cell recording mode, the inhibition both by β-carbolines and by picrotoxin decreased when hippocampal neurons got older in culture (Fig. 5, A–D). For picrotoxin (Fig. 5, A and B), the IC_{50} was 0.37 ± 0.05 μM, and the maximal inhibition was 12.6 ± 1.7% of control ($n = 4$–7) at 2 to 3 DIV and changed to 2.40 ± 0.44 μM and 22.1 ± 3.9% of control ($n = 4$–13) at 10 to 17 DIV ($P < 0.001$; ANOVA-2). For β-carbolines, we also observed a change with culture age in their blocking property of GlyRs. For βCCB (Fig. 5, C and D), the IC_{50} and the maximal inhibition were 0.8 ± 0.2 μM and 39.7 ± 8.0% of control ($n = 5$–16) at <4 DIV and 2.3 ± 1.6 μM and 73.2 ± 3.3% of control ($n = 4$–11) at >7 DIV, respectively ($P < 0.001$; ANOVA-2). A similar shift was obtained with DMCM (data not shown) for which the IC_{50} and the maximal inhibition were 2.8 ± 1.4 μM and 53.1 ± 7.1% of control ($n = 4$–33) at <4 DIV and 0.9 ± 0.9 μM and 83.2 ± 3.5% of control ($n = 5$–9) at >7 DIV, respectively ($P < 0.001$; ANOVA-2).

RT-PCR amplification of GlyR subunit mRNAs from cul-

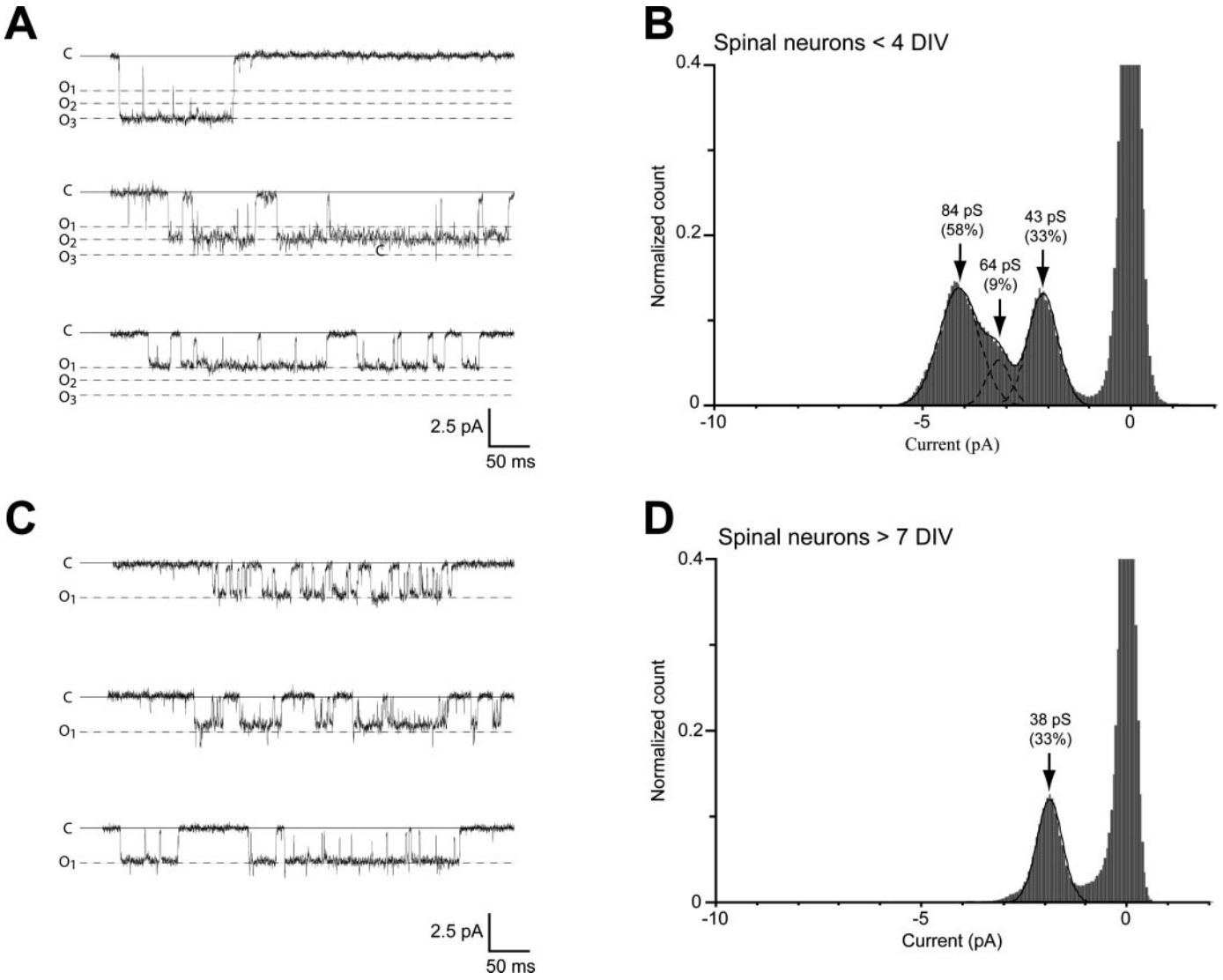

Fig. 2. Distinct repartition of GlyR conductance levels between immature and mature spinal cord neurons. A and C, examples of unitary currents evoked by application of 100 μM glycine on outside-out patches excised from 2 to 3 DIV (A) and 11 to 14 DIV (C) spinal neurons (holding potential −50 mV). The closed state C is marked by a continuous line. Conductance levels detected in the all-point histograms shown in B and D are indicated by dotted line and labeled from the lowest conductance level O1 to the highest O3. Traces were sampled at 20 kHz and filtered at 2 kHz and correspond to epochs from longer recordings obtained from different patches. B and D, point-per-point amplitude histograms of unitary currents evoked by 100 μM glycine applied on outside-out patches excised from 2 to 3 DIV (B) and 11 to 14 DIV (D) spinal neurons. The amplitude histogram was obtained by pooling recorded epochs of 25 to 50 s from nine (B) and eight (D) patches. The amplitude histogram was best fitted by the sum of three (B) or by only one (D) Gaussian functions. The mean conductances and the relative areas are indicated for each Gaussian function. The conductance was determined from the mean amplitude of each Gaussian function with $E_{Cl} = -2$ mV (holding potential −50 mV). The amplitude histograms were normalized using the current amplitude distribution corresponding to the baseline. The width of a single bar is 0.05 pA.

tured hippocampal neurons (Fig. 5E) showed that although no α1 is expressed whatever the culture time period, both immature and mature hippocampal neurons express α2, α3, and β subunit transcripts. In spite of the fact that the single-channel recordings and the picrotoxin sensitivity clearly demonstrate an increase in the heteromeric/homomeric GlyRs between <4 and >7 DIV, we thus cannot exclude that the decrease in β-carboline sensitivity of GlyRs could be caused by an increase in the α3 subunit expression level in hippocampal neurons (Fig. 5E).

Characterization of α2 Homomeric and α2β Heteromeric GlyRs Stably Expressed in CHO Cells. To determine whether the decrease in β-carboline sensitivity of GlyRs in cultured spinal cord and hippocampal neurons could mainly be caused, as is known for picrotoxin, by an increase in GlyR β subunit expression, the effects of β-carbolines on

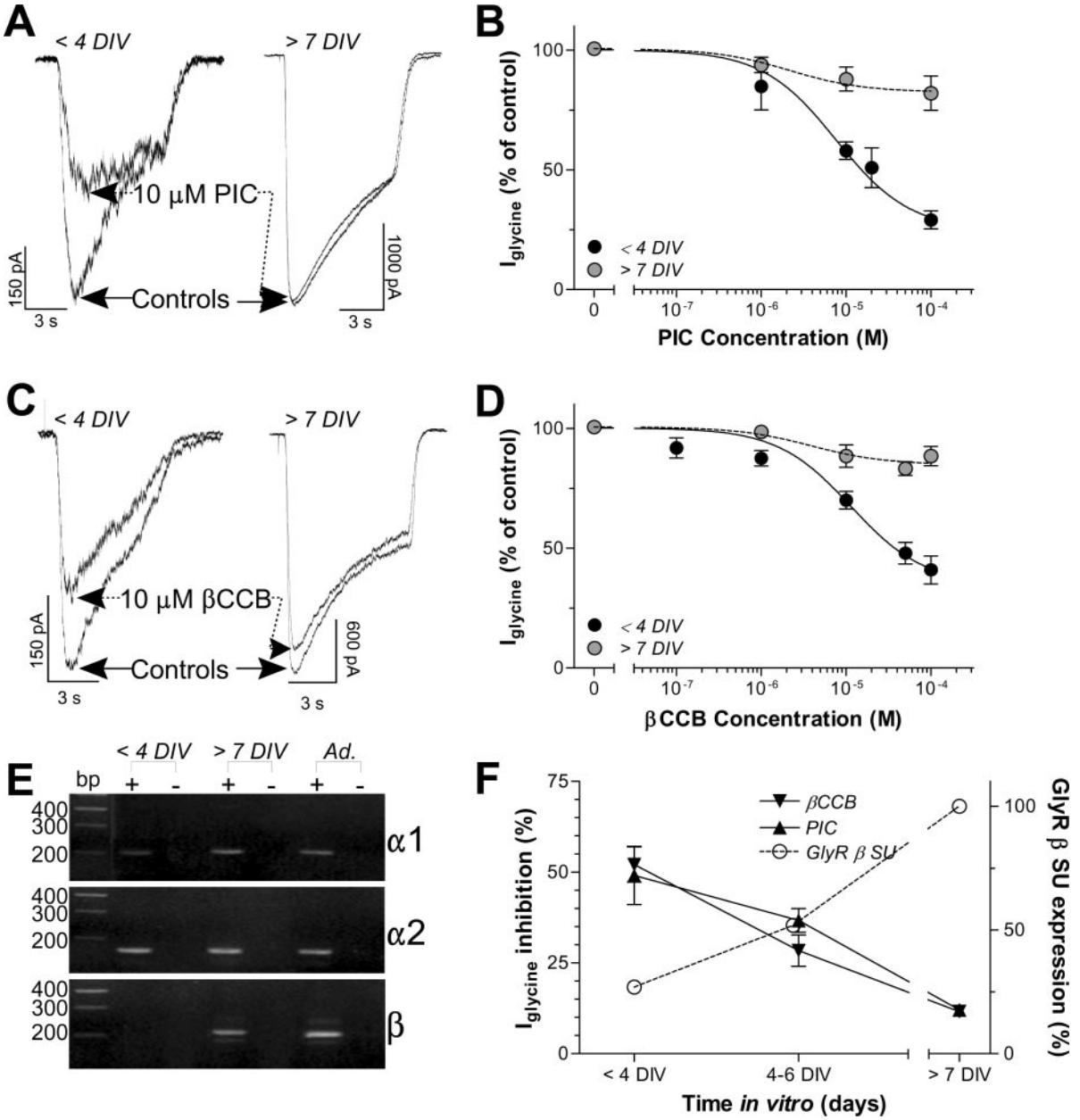

Fig. 3. Spinal cord neuron GlyR subunit composition and pharmacology are culture time-dependent. A and C, 2 to 3 (<4 DIV) and 8 to 15 (>7 DIV) DIV spinal cord neurons were perfused for 10 s with 100 μM glycine alone or in combination with 10 μM picrotoxin (PIC; A) or 10 μM βCCB (C). A 15-s pretreatment of the drugs was done, and a 60-s period was allowed for the washout of the drugs. B and D, currents elicited by 100 μM glycine in <4 DIV and in >7 DIV spinal cord neurons were recorded for increasing picrotoxin (PIC; B) or βCCB (D) concentrations. Results are expressed as percentage of glycine-induced currents peak amplitudes in the absence of any drug (mean ± S.E.M., n = 3–10 for <4 DIV, B; n = 3–5 for >7 DIV, B; n = 3–15 for <4 DIV, D; and n = 4–5 for >7 DIV, D). E, RT-PCR amplification of GlyR α1, α2, and β subunit transcripts in total RNA extracted from 2 to 3 (<4 DIV) and 8 to 15 (>7 DIV) DIV-cultured spinal cord neurons and adult mouse brain tissue (Ad.). Signals corresponding to α1 (211 bp), α2 (182 bp), and β (228 bp) were detected (+, with reverse transcriptase; −, negative controls without reverse transcriptase to exclude a possible genomic DNA contamination of RNA preparation). Left margins indicate migration of standard DNA markers the size of which is indicated in base pairs. F, picrotoxin (PIC) and βCCB inhibition of glycine-induced currents recorded in spinal cord neurons (left ordinate axis) and the level of β subunit transcript expression detected by quantitative RT-PCR (right ordinate axis) are expressed as a function of culture time. For glycine-induced currents, results are expressed as 100% of glycine-induced currents peak amplitudes in the absence of any drug (mean ± S.E.M.; n = 10).

glycine-evoked currents were analyzed on CHO cells permanently transfected either with the GlyR α2 subunit alone or in combination with the β subunit.

The quality of the transfection was checked in cloned cells by several experimental approaches. First, total RNA extracted from wild-type, GlyR-α2, and GlyR-α2+β CHO cultures were reverse-transcribed and amplified with primers specific for α2 and β (Table 1). This procedure disclosed signals for α2 in the two sets of transfected cells and a signal for β in GlyR-α2+β CHO cultures only (Fig. 6A). Corresponding signals were never found in wild-type CHO cells (Fig. 6A). Second, CHO cultures were labeled with anti-GlyR mAb4a antibodies that revealed that GlyRs were expressed at the protein level in transfected cells (Fig. 6B), whereas they were absent from wild-type CHO cells (data not shown). Third, the presence of functional GlyRs was assessed by whole-cell patch-clamp electrophysiological recordings. Figure 6C illustrates typical responses elicited by 1 mM glycine in cultured wild-type, GlyR-α2, and GlyR-α2+β CHO cells. Glycine responses of recombinant CHO cells were reversibly inhibited by strychnine (data not shown). The glycine EC_{50} and Hill coefficient of glycine-evoked response was 199 $\pm$ 31 μM and 1.8 in GlyR-α2 CHO cells (n = 7) and 62.3 $\pm$ 10.6 μM and 1.8 in GlyR-α2+β CHO cells (n = 4).

Functional properties of GlyR subtypes expressed in GlyR-α2 and GlyR-α2+β CHO cells were then studied at the single-channel level in outside-out patches excised from both cell lineages. In this model, true comparisons are allowed because the cell clones have been sequentially generated (i.e., the β subunit has been transfected in GlyR-α2 clones), which thus overcomes the classic problem of the variable degree of

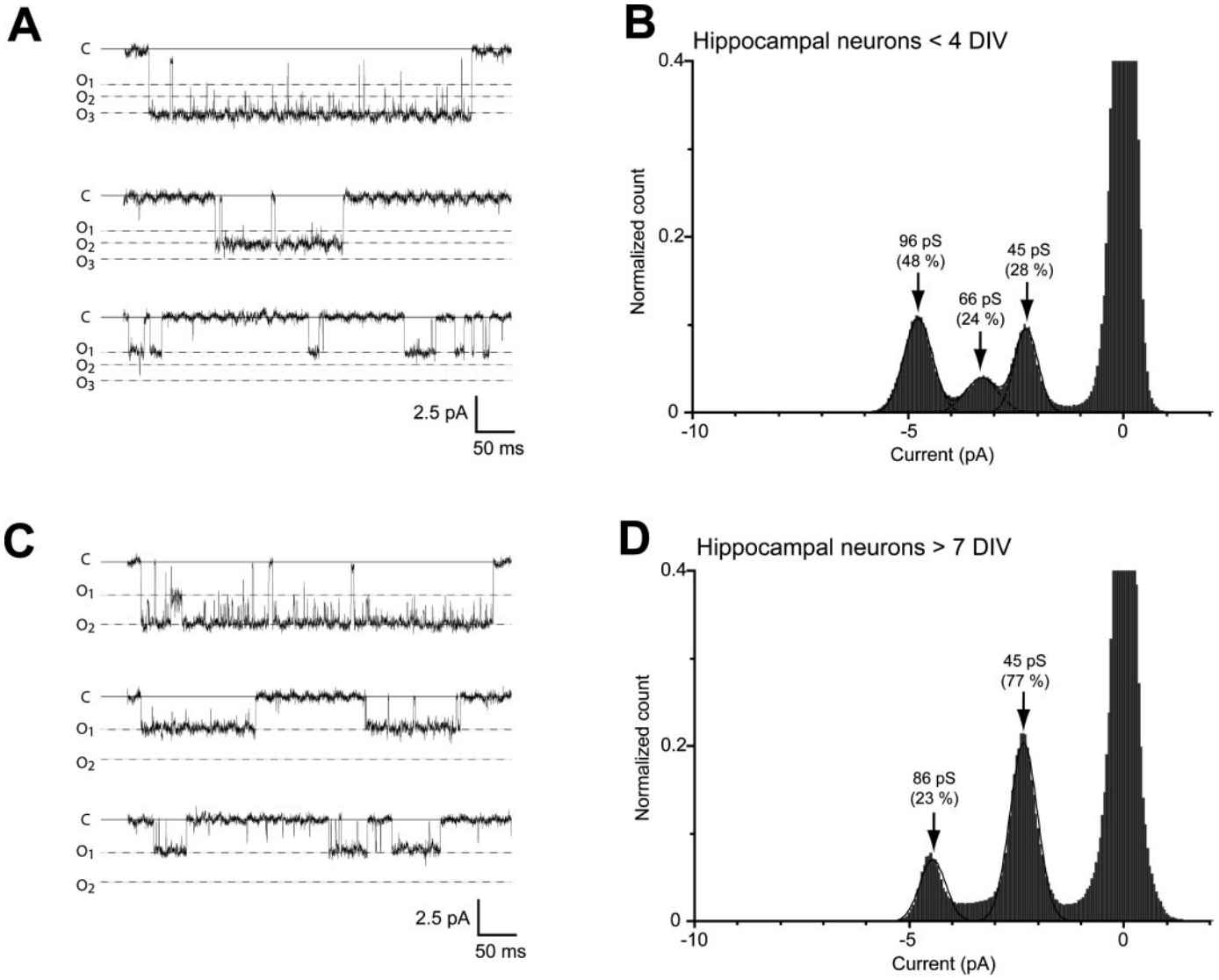

Fig. 4. Distinct repartition of GlyR conductance levels between immature and mature hippocampal neurons. A and C, examples of unitary currents evoked by application of 100 μM glycine on outside-out patches excised from 2 to 3 DIV (A) and 11 to 14 DIV (C) hippocampal neurons (holding potential $-$50 mV). The closed state C is marked by a continuous line. The conductance levels detected in the all-point histogram shown in B and D are indicated by dotted line and labeled from the lowest conductance level O1 to the highest O3. Traces were sampled at 20 kHz and filtered at 2 kHz and correspond to epochs from longer recordings obtained from different patches. B and D, point-per-point amplitude histogram of unitary currents evoked by 100 μM glycine applied on outside-out patches excised from 2 to 3 DIV (B) and 11 to 14 DIV (D) hippocampal neurons. The amplitude histogram was obtained by pooling recorded epochs of 25 to 50 s from nine (B) and seven (D) patches. The amplitude histograms were best fitted by the sum of three (B) or two (D) Gaussian functions. The mean conductances and the relative areas are indicated for each Gaussian function. The conductance was determined from the mean amplitude of each Gaussian function with E_{Cl} = $-$2 mV (holding potential $-$50 mV). The amplitude histogram was normalized using the current amplitude distribution corresponding to the baseline. The width of a single bar is 0.05 pA.

expression (of α2 subunits in this case) when such a process is done in parallel. At −50 mV and with equimolar intra- and extracellular Cl^- concentrations, unitary currents evoked by glycine in GlyR-α2 and GlyR-α2+β CHO cells exhibited multiple conductance levels (Fig. 7A). In GlyR-α2 CHO cells, the all-point amplitude histogram of GlyR unitary currents exhibited four conductance peaks at 106, 92, 62, and 45 pS (Fig. 7B). The 106- and 92-pS levels were most frequently observed and represent 36 and 52% of the total open time (Fig. 7B; n = 11), respectively. In GlyR-α2+β CHO cells (Fig. 7C; n = 13), the relative proportion of the various conductance levels was greatly modified: the two lowest conductance levels detected at 54-pS (36% of the total open time) and 22-pS level (24%) became predominant upon the higher conductance levels detected at 103 pS (23%) and 92 pS (17%).

The increase in the relative occurrence of the low conductance levels (<55 pS) from 12 to 60% between GlyR-α2 and GlyR-α2+β CHO cells confirms the expression of functional

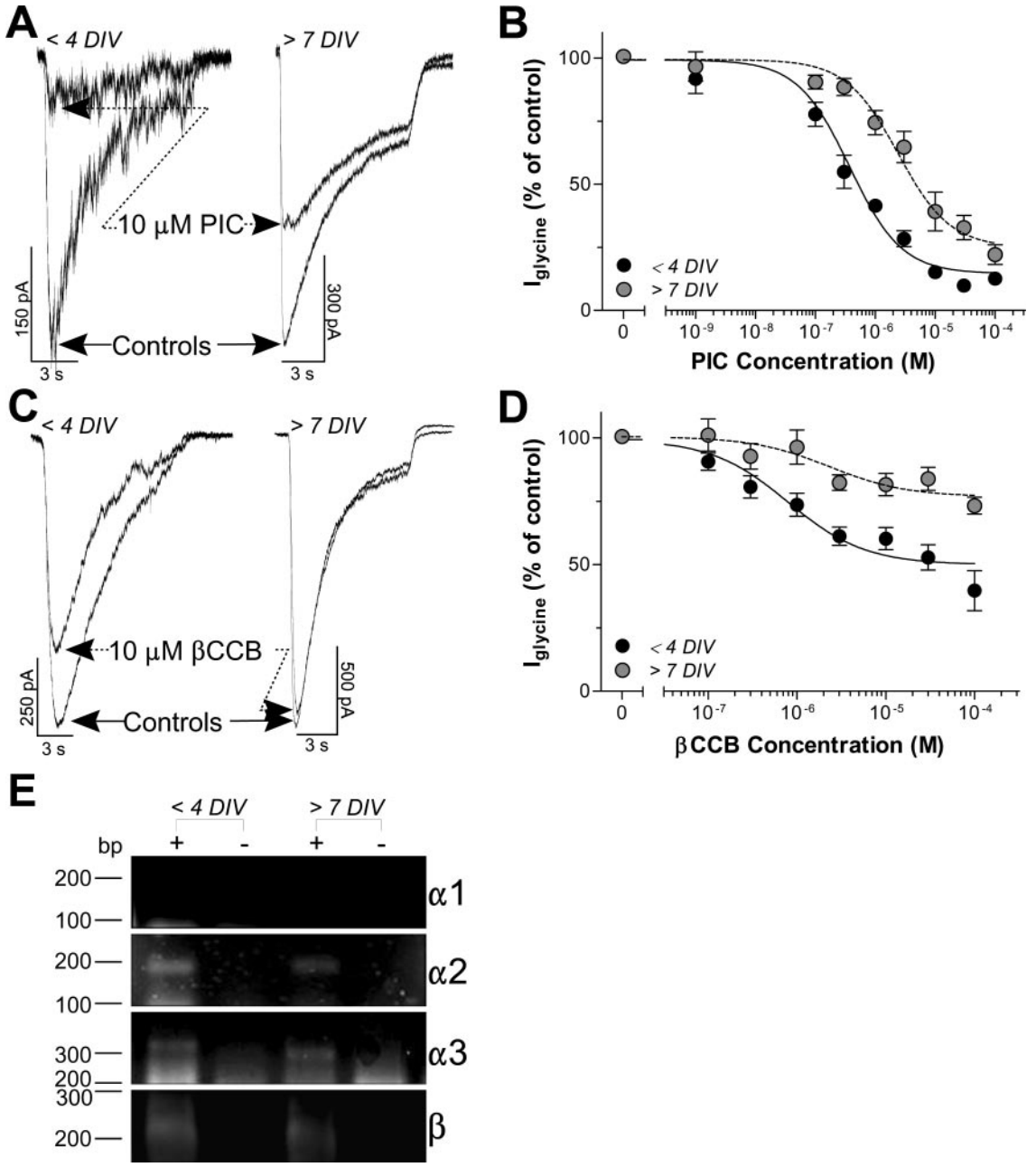

Fig. 5. βCCB and picrotoxin inhibition of glycine-gated currents in cultured hippocampal neurons. A and C, 2 to 3 (<4 DIV) and 10 to 17 (>7 DIV) DIV hippocampal neurons were perfused for 10 s with 100 μM glycine alone or in combination with 10 μM picrotoxin (PIC; A) or 10 μM βCCB (C). A 15-s pretreatment of the drugs was done, and a 60-s period was allowed for the washout of the drugs. B and D, currents elicited by 100 μM glycine in <4 DIV and in >7 DIV hippocampal neurons were recorded for increasing picrotoxin (PIC; B) or βCCB (D) concentrations. Results are expressed as percentage of glycine-induced currents peak amplitudes in the absence of any drug (mean ± S.E.M., n = 3–7 for <4 DIV, B; 4–13 for >7 DIV, B; 5–16 for <4 DIV, D; and 4–11 for >7 DIV, D). E, RT-PCR amplification of GlyR α1, α2, α3, and β subunit transcripts in total RNA extracted from 2 to 3 (<4 DIV) and 10 to 17 (>7 DIV) DIV cultured hippocampal neurons. No signal corresponding to α1 (211 bp), but well signal corresponding to α2 (182 bp), α3 (309 bp), and β (228 bp) were detected (+, with reverse transcriptase; –, negative controls without reverse transcriptase). Left margins indicate migration of standard DNA markers the size of which is indicated in base pairs.

$\alpha 2\beta$ heteromeric GlyR in the latter cell lineage. Nevertheless, the presence of higher conductance levels (>55 pS) in GlyR-$\alpha 2+\beta$ CHO cells suggested the persistence of a $\alpha 2$ homomeric GlyR expression.

Picrotoxin and β-Carboline Sensitivity of Recombinant GlyRs. The relative proportion of high conductance levels (>55 pS) between GlyR-$\alpha 2$ and GlyR-$\alpha 2+\beta$ CHO cells suggests that ~50% of the GlyRs expressed by GlyR-$\alpha 2+\beta$ CHO cells are heteromeric. This was confirmed by whole-cell patch-clamp measurements of the inhibition by picrotoxin of glycine-gated currents in both cell types (Fig. 8A). The concentration-response curves of picrotoxin inhibition (Fig. 8B) both differ in their IC_{50} (0.8 ± 0.1 μM, n = 3–47 for GlyR-$\alpha 2$ and 1.6 ± 0.4 μM, n = 8–76 for GlyR-$\alpha 2+\beta$; $P < 0.001$; ANOVA-2) and their maximal measured inhibition at 100 μM (5.7 ± 1.1% of control, n = 36 for GlyR-$\alpha 2$ compared with 21.2 ± 2.3% of control, n = 76 for GlyR-$\alpha 2+\beta$).

Next, the effects of βCCB on the glycine responses of both transfected CHO cells were assessed. Figure 8, C and D, demonstrates the highly significant difference in βCCB-induced inhibition between GlyR-$\alpha 2$ and GlyR-$\alpha 2+\beta$ CHO cells. The former had a βCCB IC_{50} of 0.9 ± 0.2 μM and a maximal blocking effect of 43.9 ± 3.0% of control (n = 6–12), and the latter had an IC_{50} of 0.3 ± 0.3 μM and a maximal inhibition of 80.5 ± 4.5% of control (n = 7–28; $P < 0.001$; ANOVA-2).

Finally, the question arose as to with which site on the GlyR could βCCB interact. We first looked for a competition with picrotoxin because βCCB showed a similar developmental- and GlyR subunit-dependent effect. Therefore, we measured the inhibitions of glycine-gated currents by 10 μM βCCB and 10 μM picrotoxin alone or in combination on the glycine responses of GlyR-$\alpha 2$ CHO cells. Figure 8E demonstrates the additivity of their effects (44.0 ± 6.2% of inhibition for βCCB alone compared with 69.3 ± 5.4% for both compounds together; n = 5; $P < 0.05$; ANOVA-1), hence ruling out that picrotoxin and βCCB share a common site and/or mechanism of inhibition of GlyR function. Second, we checked for the recently described low-affinity site for benzodiazepine (Thio et al., 2003) by measuring the interaction of 10 μM βCCB with 10 μM Ro 15-1788 (flumazenil), the prototypic benzodiazepine antagonist at $GABA_A$Rs. As shown in Fig. 8F, flumazenil reversed the inhibition of glycine currents by βCCB to control level (9.6 ± 0.7% of inhibition with both drugs compared with 29.6 ± 2.9% for βCCB alone; n = 8; $P <$ 0.001; ANOVA-1).

Discussion

In this work, we have shown that β-carboline inhibition is only observed in immature (<4 DIV) cultured spinal cord and hippocampal neurons, predominantly expressing α homo-

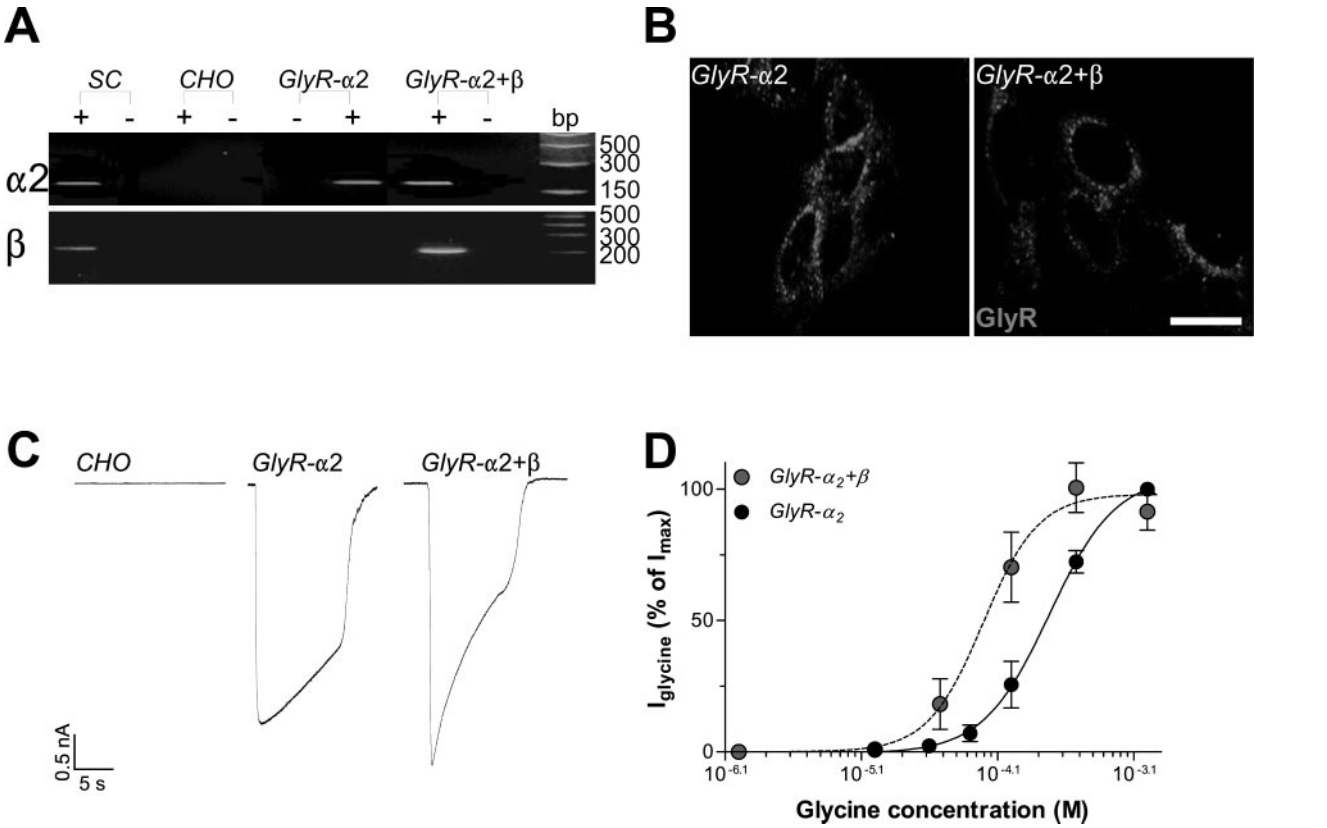

Fig. 6. Morphofunctional characterization of GlyRs expressed by transfected GlyR-$\alpha 2$ and GlyR-$\alpha 2+\beta$ CHO cells. A, RT-PCR amplification of GlyR $\alpha 2$ and β subunit transcripts in total RNA extracted from cultured wild-type (CHO), GlyR-$\alpha 2$-transfected (GlyR-$\alpha 2$), GlyR-$\alpha 2+\beta$-transfected (GlyR-$\alpha 2+\beta$) CHO cells, and neonate mouse spinal cords (SC). Signals corresponding to $\alpha 2$ (182 bp) and β (228 bp) were detected (+, with reverse transcriptase; –, negative controls without reverse transcriptase). Right margins indicate migration of standard DNA markers the size of which is indicated in base pairs. B, confocal images of GlyR-$\alpha 2$ and GlyR-$\alpha 2+\beta$ CHO cells immunoreactive for GlyR (gray). Scale bar, 20 μm. C, currents induced by a 15-s application of 1 mM glycine in whole-cell patch-clamped and voltage-clamped (holding potential −70 mV) wild-type (CHO), GlyR-$\alpha 2$-transfected (GlyR-$\alpha 2$) and GlyR-$\alpha 2+\beta$-transfected (GlyR-$\alpha 2+\beta$) CHO cells. D, concentration-response curves of currents evoked by increasing glycine concentrations were recorded in GlyR-$\alpha 2$ (black dots) and in GlyR-$\alpha 2+\beta$ (gray dots) CHO cells. Results are expressed as percentage of currents induced by 1 mM glycine (mean ± S.E.M., n = 7 for GlyR-$\alpha 2$ and 4 for GlyR-$\alpha 2+\beta$).

meric GlyRs. Mature (>7 DIV) neuron insensitivity to β-carbolines paralleled their insensitivity to picrotoxin and was correlated with the replacement of α homomeric by αβ heteromeric GlyRs in both cell types. We definitely conclude that the expression of β subunits is sufficient to account for the disappearance of β-carboline inhibition by comparing the pharmacological profiles of CHO cells stably transfected with GlyR-α2 and GlyR-α2+β subunits. We also report, for the first time, that cultured hippocampal neurons undergo, like spinal cord neurons, a developmental regulation of their GlyR properties during in vitro maturation.

β-Carbolines Are Antagonists of α_2 Homomeric GlyRs. Pharmacological agents have been invaluable tools to study ion channel function. Available drugs that could help us study strychnine-sensitive GlyRs, however, are much less abundant than, for example, those for $GABA_A$Rs (Laube, 2002). So far, picrotoxin (Lynch et al., 1995), and more recently some quinoxalines (Meier and Schmieden, 2003), are the only known pharmacological tools able to discriminate between homomeric and heteromeric GlyRs. Here, we report that β-carbolines, which are known benzodiazepine inverse agonists at $GABA_A$Rs, can also fulfill such a role. In spinal neurons, the amount of blockade induced by the two inhibitors remains very close, and both of them easily discriminate between immature and mature spinal GlyRs. By contrast, in hippocampal neurons and transfected CHO cells, βC seems to be a better tool than picrotoxin to detect the partial homomer/heteromer switch observed in these cells. Indeed, for picrotoxin, we mainly observed a slight shift in the IC_{50}, whereas both IC_{50} and maximal inhibition were affected for β-carbolines Therefore, a complete concentration-inhibition curve should be needed to document the switch with picrotoxin, whereas a single inhibition assay at a high β-carboline concentration (>10 μM) would be sufficient to estimate the ratio homomer/heteromer.

In our models, picrotoxin inhibition of GlyRs paralleled that of β-carbolines, raising the question of a common binding site on α2 homomeric GlyRs. This is very unlikely, how-

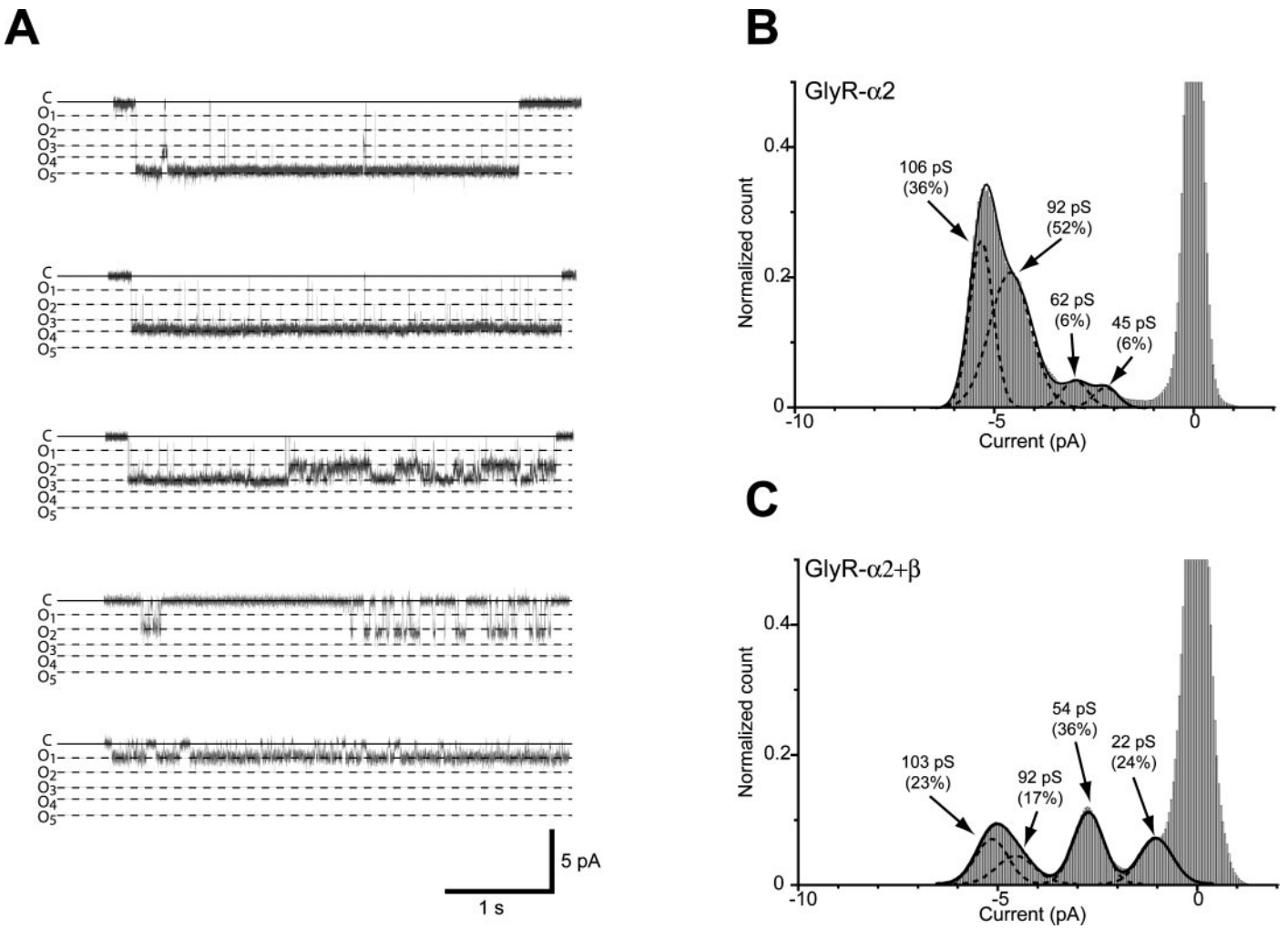

Fig. 7. Distinct repartition of GlyR conductance levels between GlyR-α2 and GlyR-α2+β CHO cells. A, examples of unitary currents evoked by 100 μM glycine applied on outside-out patches excised from GlyR-α2 or GlyR-α2+β CHO (holding potential −50 mV). The closed state C is indicated by a continuous line, whereas open states are indicated by a dotted line and labeled from the lowest level O1 to the highest level O5. Traces were sampled at 25 kHz and filtered at 1 kHz and correspond to epochs from longer recordings obtained from different patches. B and C, point-per-point amplitude histograms of unitary currents evoked by 100 μM glycine applied on outside-out patches excised from GlyR-α2 (B) and GlyR-α2+β (C) CHO cells. The amplitude histograms shown in B and C were obtained by pooling recorded epochs of 50 s from 11 and 13 patches, respectively. Amplitude histograms were best fitted by the sum of four Gaussian functions. The mean conductances and the relative areas are indicated for each Gaussian function. Conductance levels were determined from the mean amplitude of each Gaussian function with $E_{Cl} = -2$ mV (holding potential −50 mV). Amplitude histograms were normalized using the current amplitude distribution corresponding to the baseline. The width of a single bar is 0.1 pA.

ever, because the inhibitions by β-carbolines and picrotoxin are additive. Concerning the putative GlyR binding site for β-carbolines, when we first reported β-carboline inhibition of GlyRs in immature cultured spinal cord neurons and its reversal by some antiepileptic drugs (Rigo et al., 2002), we suggested that it could be mediated by a low-affinity benzodiazepine site common to GlyR and $GABA_AR$ described previously (Walters et al., 2000). This hypothesis was recently reinforced by the finding that some benzodiazepines inhibit glycine responses of α2-containing GlyRs from cultured hippocampal neurons (Thio et al., 2003). Our observed reversal of β-carboline inhibition by flumazenil, a benzodiazepine antagonist at $GABA_ARs$, further supports this hypothesis.

In Vitro Maturation of GlyRs in Spinal Cord and Hippocampal Neurons. Supported by morphological as well as functional arguments, several reports have documented the developmental switch in GlyR subunit expression (embryonic-neonatal α2 homomers–juvenile α2β hetero-

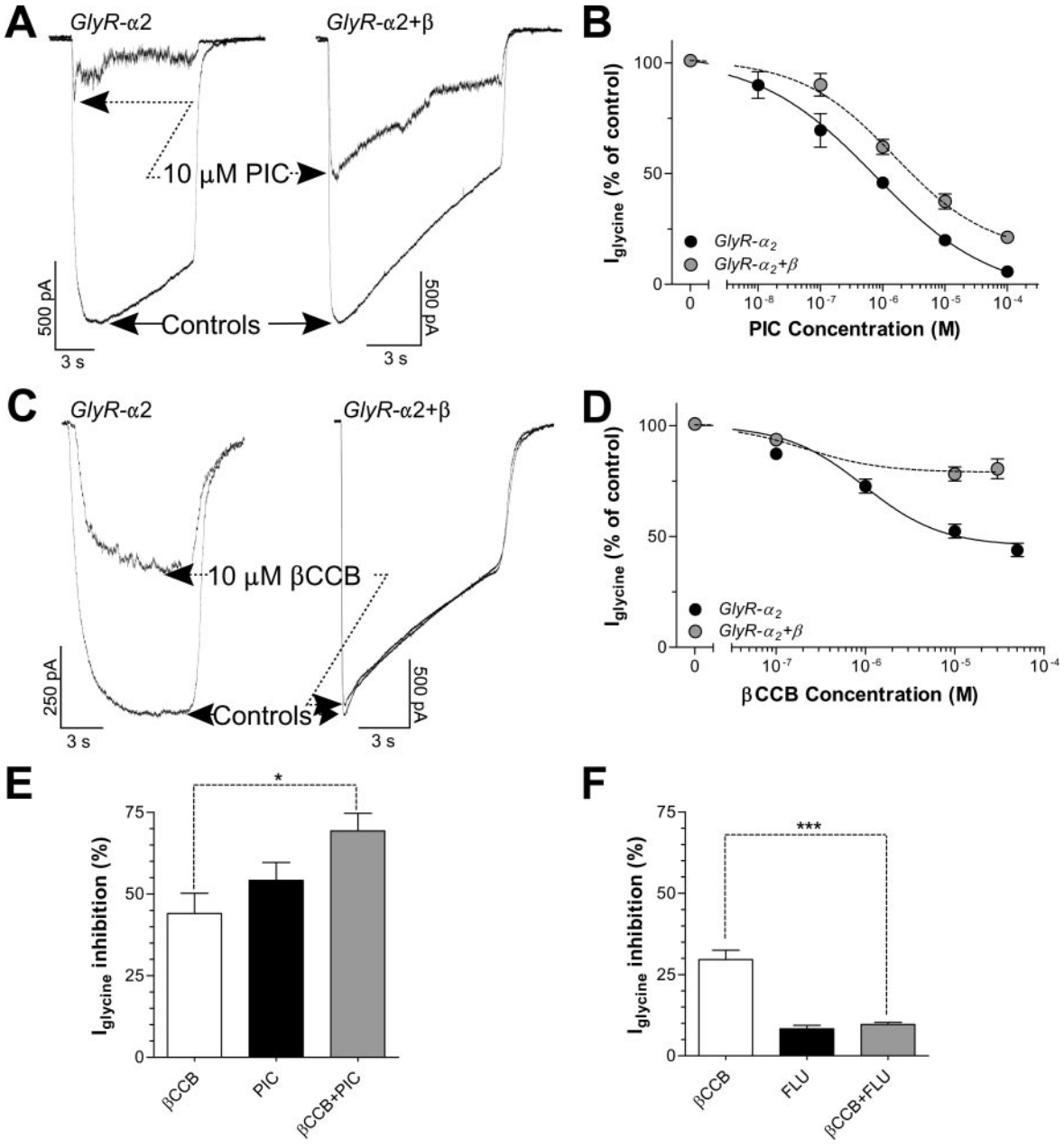

Fig. 8. βCCB and picrotoxin sensitivity of GlyR-α2 and GlyR-α2+β CHO cells. A and C, GlyR-α2 and GlyR-α2+β CHO cells were perfused for 10 s with 100 μM glycine alone or in combination with 10 μM picrotoxin (PIC; A) or 10 μM βCCB (C). A 15-s pretreatment of the drugs was done, and a 60-s period was allowed for the washout of the drugs. B and D, currents elicited by 100 μM glycine in GlyR-α2 and in GlyR-α2+β CHO cells were recorded for increasing picrotoxin (PIC; B) or βCCB (D) concentrations. Results are expressed as percentage of glycine-induced currents peak amplitudes in the absence of any drug (mean ± S.E.M., n = 3–47 for GlyR-α2, B; 5–29 for GlyR-α2+β, B; 6–17 for GlyR-α2, D; and 7–28 for GlyR-α2+β, D). E, currents elicited by 100 μM glycine in GlyR-α2 CHO cells were recorded in the presence of either 10 μM βCCB or picrotoxin (PIC) alone or in combination. Results are expressed as a hundred minus percentage of glycine-induced currents peak amplitudes in the absence of any drug (mean ± S.E.M., n = 4–5; *, $P < 0.05$, one-way analysis of variance followed by Dunnett's post tests). F, currents elicited by 100 μM glycine in 3 DIV spinal cord neurons were recorded in the presence of either 10 μM βCCB or flumazenil (FLU) alone or in combination. Results are expressed as a hundred minus percentage of glycine-induced currents peak amplitudes in the absence of any drug (mean ± S.E.M., n = 6–8; ***, $P < 0.001$, one-way analysis of variance followed by Dunnett's post tests).

mers–adult α1β heteromers) underlying the change in glycinergic transmission that occurs, both in vitro and in vivo, in spinal cord and brainstem neurons (Withers and St John, 1997; Singer et al., 1998; Tapia and Aguayo, 1998; Singer and Berger, 2000). Here, combining quantitative RT-PCR and single-channel recordings, we further characterize this developmental schedule by showing that the appearance of functional αβ heteromers during the in vitro maturation of spinal cord neurons is caused, at least in part, by a transcriptional regulation of the β subunit expression.

As already mentioned in the introduction, GlyRs are also known to be expressed in more rostral regions of the central nervous system. The exact subunit composition of the GlyRs expressed in those regions is poorly documented, and, so far, no true developmental regulation, as the one that occurs in the spinal cord, has been described. Our study clearly shows that GlyRs expressed by hippocampal neurons undergo such a developmental regulation during in vitro maturation. However, this maturation process differs from spinal neurons in several aspects. First, the persistence of high conductance levels in 11 to 14 DIV hippocampal neurons shows that the replacement of homomers by heteromers is not complete at this time. Such a persistence of homomeric GlyRs is also supported by the higher β-carboline and picrotoxin sensitivity of glycine-evoked currents in mature hippocampal neurons compared with mature spinal neurons. This observation could result from a slower maturation process in hippocampal neurons. However, homomeric GlyRs are known to be expressed by mature hippocampal neurons recorded in 4-week-old rat brain slices, supporting the hypothesis of a partial maturation process in hippocampal neurons (Chattipakorn and McMahon, 2002).

RT-PCR experiments show that no qualitative change of GlyR subunits occurred during the in vitro maturation of hippocampal neurons: at least at the transcript level, α2, α3, and β subunits were present from the beginning of the culture period. Although no α2-to-α1 subunit switch occurs in hippocampal neurons, one can hypothesize an alternative α2-to-α3 switch. However, we observed very similar pharmacological properties between <4 DIV hippocampal neurons and GlyR-α2 CHO cells on the one hand and between >7 DIV hippocampal neurons and GlyR-α2+β CHO cells on the other hand. Because the ratio of high (>55 pS) versus low (<55 pS) conductance levels is similar in both cases, we can speculate that either α2-contaning GlyRs have the same pharmacological properties than α3-containing GlyRs or that the α3 subunit is poorly expressed in hippocampal neurons. The latter hypothesis could explain the fact that Thio et al. (2003) were unable to detect α3 subunit transcript in 4 to 14 DIV hippocampal neurons.

Pathophysiological and Physiological Implications. A still unresolved question concerns the actual existence of endogenous allosteric modulators of ligand-gated channels. In that respect, and regarding inhibitory receptors, almost only zinc (Barberis et al., 2000; Suwa et al., 2001) and protons (Chen et al., 2004) were conclusively demonstrated as endogenous modulators. Some β-carbolines (e.g., βCCB used in this study) were also proposed as endogenous compounds, but this has not been studied further for more than 10 years (Braestrup et al., 1980; Medina et al., 1989). To what extent these modulators actually influence neurotransmission or other inhibitory receptor-mediated effects remains largely unknown.

Extrasynaptic homomeric α2-containing GlyRs have been described in the adult brain where they have been proposed to participate in the tonic regulation of excitability (Mori et al., 2002; Chattipakorn and McMahon, 2003), hence being interesting targets for excitability disorders, such a epilepsy. In that respect, it has been demonstrated that some antiepileptic drugs (e.g., levetiracetam) are able to reverse both β-carboline- and zinc-induced inhibition not only of $GABA_A$Rs but also of GlyRs (Rigo et al., 2002). GlyRs have also been proposed to participate in developmental processes (Flint et al., 1998) and, more recently, α2-containing GlyRs have even been described in progenitors of rod photoreceptor in the retina (Young and Cepko, 2004). Hence, further characterizing the properties and the roles of immature GlyRs certainly deserves attention.

Acknowledgments

We thank P. Ernst-Gengoux, A. Brose, P. Coucke, and C. Mazy-Servais for technical support and expertise.

References

Barberis A, Cherubini E, and Mozrzymas JW (2000) Zinc inhibits miniature GABAergic currents by allosteric modulation of GABAA receptor gating. *J Neurosci* **20:**8618–8627.
Beato M, Groot-Kormelink PJ, Colquhoun D, and Sivilotti LG (2004) The activation mechanism of alpha1 homomeric glycine receptors. *J Neurosci* **24:**895–906.
Becker CM, Hoch W, and Betz H (1988) Glycine receptor heterogeneity in rat spinal cord during postnatal development. *EMBO (Eur Mol Biol Organ) J* **7:**3717–3726.
Bormann J, Rundstrom N, Betz H, and Langosch D (1993) Residues within transmembrane segment M2 determine chloride conductance of glycine receptor homo- and hetero-oligomers. *EMBO (Eur Mol Biol Organ) J* **12:**3729–3737.
Braestrup C, Nielsen M, and Olsen CE (1980) Urinary and brain B-carboline-3-carboxylates as potent inhibitors of brain benzodiazepine receptors. *Proc Natl Acad Sci USA* **77:**2288–2292.
Chattipakorn SC and McMahon LL (2002) Pharmacological characterization of glycine-gated chloride currents recorded in rat hippocampal slices. *J Neurophysiol* **87:**1515–1525.
Chattipakorn SC and McMahon LL (2003) Strychnine-sensitive glycine receptors depress hyperexcitability in rat dentate gyrus. *J Neurophysiol* **89:**1339–1342.
Chen Z, Dillon GH, and Huang R (2004) Molecular determinants of proton modulation of glycine receptors. *J Biol Chem* **279:**876–883.
Flint AC, Liu X, and Kriegstein AR (1998) Nonsynaptic glycine receptor activation during early neocortical development. *Neuron* **20:**43–53.
Hogg RC, Chipperfield H, Whyte KA, Stafford MR, Hansen MA, Cool SM, Nurcombe V, and Adams DJ (2004) Functional maturation of isolated neural progenitor cells from the adult rat hippocampus. *Eur J Neurosci* **19:**2410–2420.
Laube B (2002) Potentiation of inhibitory glycinergic neurotransmission by Zn^{2+}: a synergistic interplay between presynaptic P2X2 and postsynaptic glycine receptors. *Eur J Neurosci* **16:**1025–1036.
Laube B, Maksay G, Schemm R, and Betz H (2002) Modulation of glycine receptor function: a novel approach for therapeutic intervention at inhibitory synapses? *Trends Pharmacol Sci* **23:**519–527.
Legendre P (2001) The glycinergic inhibitory synapse. *Cell Mol Life Sci* **58:**760–793.
Leprince P, Lefebvre PP, Rigo J-M, Delrée P, Rogister B, and Moonen G (1989) Cultured astroglia release a neuronotoxic activity that is not related to the excitotoxins. *Brain Res* **502:**21–27.
Lynch JW, Rajendra S, Barry PH, and Schofield PR (1995) Mutations affecting the glycine receptor agonist transduction mechanism convert the competitive antagonist, picrotoxin, into an allosteric potentiator. *J Biol Chem* **270:**13799–13806.
Malosio ML, Marqueze-Pouey B, Kuhse J, and Betz H (1991) Widespread expression of glycine receptor subunit MRNAs in the adult and developing rat brain. *EMBO (Eur Mol Biol Organ) J* **10:**2401–2409.
Mangin JM, Baloul M, Prado DC, Rogister B, Rigo JM, and Legendre P (2003) Kinetic properties of the alpha2 homo-oligomeric glycine receptor impairs a proper synaptic functioning. *J Physiol (Lond)* **553:**369–386.
Mangin JM, Guyon A, Eugene D, Paupardin-Tritsch D, and Legendre P (2002) Functional glycine receptor maturation in the absence of glycinergic input in dopaminergic neurones of the rat substantia nigra. *J Physiol (Lond)* **542:**685–697.
McCool BA and Farroni JS (2001) Subunit composition of strychnine-sensitive glycine receptors expressed by adult rat basolateral amygdala neurons. *Eur J Neurosci* **14:**1082–1090.
Medina JH, de Stein ML, and De Robertis E (1989) *N*-[^{3}H]Butyl-β-carboline-3-carboxylate, a putative endogenous ligand, binds preferentially to subtype 1 of central benzodiazepine receptors. *J Neurochem* **52:**665–670.
Meier J and Schmieden V (2003) Inhibition of alpha-subunit glycine receptors by quinoxalines. *Neuroreport* **14:**1507–1510.
Mori M, Gahwiler BH, and Gerber U (2002) beta-Alanine and taurine as endogenous

agonists at glycine receptors in rat hippocampus in vitro. *J Physiol (Lond)* **539:** 191–200.
Moss SJ and Smart TG (2001) Constructing inhibitory synapses. *Nat Rev Neurosci* **2:**240–250.
Nguyen L, Malgrange B, Belachew S, Rogister B, Rocher V, Moonen G, and Rigo J-M (2002) Functional glycine receptors are expressed by postnatal nestin positive neural stem/progenitor cells. *Eur J Neurosci* **15:**1299–1305.
Ortells MO and Lunt GG (1995) Evolutionary history of the ligand-gated ion-channel superfamily of receptors. *Trends Neurosci* **18:**121–127.
Rigo J-M, Coucke P, Rogister B, Belachew S, Mazy-Servais C and Moonen G (1998) β-Carbolines: negative allosteric modulators of GABA- and glycine-gated chloride channels. *Soc Neurosci Abstr* **24:**1759.
Rigo JM, Hans G, Nguyen L, Rocher V, Belachew S, Malgrange B, Leprince P, Moonen G, Selak I, Matagne A, et al. (2002) The anti-epileptic drug levetiracetam reverses the inhibition by negative allosteric modulators of neuronal. *Br J Pharmacol* **136:**659–672.
Schrader N, Kim EY, Winking J, Paulukat J, Schindelin H, and Schwarz G (2004) Biochemical characterization of the high affinity binding between the glycine receptor and gephyrin. *J Biol Chem* **279:**18733–18741.
Sergeeva OA and Haas HL (2001) Expression and function of glycine receptors in striatal cholinergic interneurons from rat and mouse. *Neuroscience* **104:**1043–1055.
Singer JH and Berger AJ (2000) Development of inhibitory synaptic transmission to motoneurons. *Brain Res Bull* **53:**553–560.
Singer JH, Talley EM, Bayliss DA, and Berger AJ (1998) Development of glycinergic synaptic transmission to rat brain stem motoneurons. *J Neurophysiol* **80:**2608–2620.
Suwa H, Saint-Amant L, Triller A, Drapeau P, and Legendre P (2001) High-affinity zinc potentiation of inhibitory postsynaptic glycinergic currents in the zebrafish hindbrain. *J Neurophysiol* **85:**912–925.
Tapia JC and Aguayo LG (1998) Changes in the properties of developing glycine receptors in cultured mouse spinal neurons. *Synapse* **28:**185–194.
Teuber L, Watjens F, and Jensen LH (1999) Ligands for the benzodiazepine binding site–a survey. *Curr Pharm Des* **5:**317–343.
Thio LL, Shanmugam A, Isenberg K, and Yamada K (2003) Benzodiazepines block alpha2-containing inhibitory glycine receptors in embryonic mouse hippocampal neurons. *J Neurophysiol* **90:**89–99.
Virginio C and Cherubini E (1997) Glycine-activated whole cell and single channel currents in rat cerebellar granule cells in culture. *Brain Res Dev Brain Res* **98:**30–40.
Walters RJ, Hadley SH, Morris KD, and Amin J (2000) Benzodiazepines act on GABAA receptors via two distinct and separable mechanisms. *Nat Neurosci* **3:**1274–1281.
Withers MD and St John PA (1997) Embryonic rat spinal cord neurons change expression of glycine receptor subtypes during development *in vitro*. *J Neurobiol* **32:**579–592.
Ye J (2000) Physiology and pharmacology of native glycine receptors in developing rat ventral tegmental area neurons. *Brain Res* **862:**74–82.
Young TL and Cepko CL (2004) A role for ligand-gated ion channels in rod photoreceptor development. *Neuron* **41:**867–879.

Address correspondence to: Dr. Jean-Michel Rigo, Department of Physiology, Transnationale Universiteit Limburg/Limburgs Universitair Centrum, Biomedisch Onderzoekinstituut, B-3590 Diepenbeek, Belgium. E-mail: jeanmichel.rigo@luc.ac.be